Egypt. J. Chem. **Vol. 66,** No. 6 pp. 205 - 216 (2023)

Egyptian Journal of Chemistry

http://ejchem.journals.ekb.eg/

Synthesis, Characterization, and Performance of New Polymeric Nonionic Surfactants as Flow Improvers and Wax Dispersants for Waxy Crude Oil

A.S. El-Tabei[1,*], T.T. Khidr [1], Amira. E. El-Tabey[1], Elsayed. A. Elsharaky[1]

[1]Egyptian Petroleum Research Institute (EPRI), Nasr City, Cairo, 11727, Egypt

Abstract

One of the major issues in waxy crude oil (WCO) production is wax deposition, which causes significant losses to the oil sector. New three polymeric nonionic surfactants (PNSs) based on 2-phenylethan-1-amine (I1, I2 & I3) were designed and synthesized in merely two simple processes (ethoxylation and esterification) to inhibit wax crystal development and enhance the cold flowability. To verify the chemical composition of the synthesized PNSs, spectroscopic analyses (FTIR, MS & NMR) were conducted, and to comprehend their attitude at the interface, interfacial tension (IFT) was investigated. The influence of a commercial additive, PNSs, and their blends on the solid point and the rheological properties of WCO were researched. The findings revealed that I3 and blend I7 delivered the highest depression in the solid point (ΔSP) at the dosage of 1000 ppm and the blend I7 performed better rheological properties than I3 in terms of enhancing oil fluidity. In comparison to a commercial additive, the synthesized PNS exhibited better solid point depression for crude oil. Also, polarizing optical microscopy was employed to explore the interaction mechanism of these PNSs with wax crystals of WCO.

Keywords: polymeric nonionic surfactants, mixed additives, solid point, rheological measurement, cold flow properties, polarizing optical microscopy.

1. Introduction

As light crude oil supplies deplete, heavy oil production, collecting and transportation have gradually increased globally **[1, 2]**. Crude oil has a complicated mixture of compounds, such as linear and branched paraffins (waxes) with varied molar masses. Due to their composition and molar mass, paraffins also have different melting points, the greater the molar mass, the melting point will be higher, and for the same carbon number, straight paraffins melt at greater temperatures than branched paraffins. The oil in the rock formation is comparatively hot and tight so that it is completely fluid. When it reaches the wellhead at the surface, a decrease in temperature and pressure is present, so the waxes (paraffins) with large molar weights undergo liquid-solid transitions, leading to the solidification of the waxes. This leads to forming aggregates of wax crystals and their deposition on the inner tube walls, which raises viscosity, decreases flow rates, and minimizes the overall production **[3–6]**.

Different mitigating strategies have been established to combat wax aggregation and deposition to enhance the low-temperature flow characteristics of WCO. These strategies may be broadly classified into two types: removing and preventing **[7,8]**. A prevention strategy was performed by using the chemical compounds defined as wax dispersants (WDs) **[9–11]**. It is the simplest practical solution to solve this issue.

Amphiphilic compounds (monomeric and polymeric) were injected as WDs at low dosages into the pipelines to prohibit paraffin wax deposition and enhance the flow characteristics of WCO at low temperatures **[12–15]**. Their alkyl chains integrate with the wax crystals whereas their polar moieties prevent the wax crystals from joining together and thus lessen the wax crystals' size **[16]**. The chemical additives (WDs) as cold flow improvers can efficiently lower the solid point (SP) of WCO via modifying the size & shape of wax crystals, allowing them to flow in cold climes **[17]**.

The focus of this research was to synthesize three polymeric nonionic surfactants (PNSs) derived from 2-phenylethan-1-amine to be employed as flow improvers and wax dispersants for WCO. These PNSs were initially synthesized via ethoxylation of 2-phenylethan-1-amine with various ethylene oxide ratios (10, 15, and 20) and the resulting ethoxylates (E10, E15, and E20) were then esterified using lauroyl chloride. Their structural composition was

Corresponding author e-mail: azizaalghalymz@yahoo.com (A.S. El-Tabei).Tel: +20 10 25761194; Fax: +20 2 22747433
Receive Date: 09 August 2022, Revise Date: 05 September 2022, Accept Date: 06 September 2022
DOI: 10.21608/EJCHEM.2022.155447.6710

verified using FTIR and ^{1}H, ^{13}C-NMR spectrum analyses. IFT measurements were conducted to assess their surface-active properties and thermodynamic parameters. The influence of commercial additive, PNSs and their blend dosages, the blends' molar ratios, and the PNSs molecular structures on the SP of WCO were tested and discussed. The rheological properties of untreated and treated WCO with commercial additive, I3, and blend I7 were measured at various temperatures. Moreover, photomicrographic analysis of treated and untreated WCO was carried out to investigate crystalline attitude as well as changes in size, shape, and aggregation of wax crystals. The depressing mechanism of the PNSs on the SP of WCO was described.

2. Materials and Experimental methods

2.1. Materials

2-phenylethan-1-amine and lauroyl chloride were supplied via Sigma-Aldrich. The ethylene oxide gas was provided by the Egyptian Gas Company. Waxy crude oil from Qarun Petroleum Company was received and utilized in the experiments. Its physicochemical characteristics were summarized in **Table1**. Gas chromatography analysis was conducted to assess the *n*-paraffin distribution of the extracted waxes according to the ASTM D 2887 standard. A commercial sample was supplied by Petrolite Chemical Company.

Table 1: Physicochemical properties of the waxy crude oil

Density @ 15°C g/ml	Viscosity (mpa.s, 50°C)	Water content vol %	Saturates (wt %)	Aromatics (wt %)	Resins (wt %)	Asphaltene (wt %)	Wax content (wt %)	n-paraffins, wt %	Iso-Paraffin, wt %	Total paraffins content, wt %
0.8652	100	0.21	51.5	26.0	21.7	0.7	10.00	82.27	7.73	90.00

2.2. Synthesis of new polymeric nonionic surfactants (PNSs)

Three new polymeric nonionic surfactants were synthesized as indicated in **Scheme 1** in two steps:

2.2.1. Ethoxylation of 2-phenylethan-1-amine

2-phenylethan-1-amine was placed in a conical flask with Na metal as a catalyst at 80°C. A stream of N_2 gas was passed throughout the system for ten minutes. Thereafter, the nitrogen stream was substituted by ethylene oxide gas (EO), which was passed regularly. Throughout the reaction time, the reaction flask was left to cool and then weighed after being flushed with nitrogen gas to investigate the quantity of EO units consumed through the ethoxylation. In accordance with the weight difference, the number of moles of EO was calculated to get three polyoxyethylene 2-phenylethan-1-amines E10, E15, and E20 with the total number of EO units (n) 10, 15, and 20 respectively. They were weighed, neutralized with HCl, dissolved in isopropyl alcohol, and salted out by a supersaturated solution of NaCl. The organic layers were extracted and isopropyl alcohol was distilled off. The resulting polyoxyethylene 2-phenylethan-1-amines were yellow viscous liquids.

2.2.2. Esterification of polyoxyethylene 2-phenylethan-1-amines

0.1 mol of Lauroyl chloride was introduced drop by drop into a conical flask containing 0.1 mol of polyoxyethylene 2-phenylethan-1-amines (E10, E15, or E20) and 0.15 mol N,N-Diethylethanamine. Dicholormethane was used as a solvent. The reaction mixtures were agitated for two hours at the temperature range from 0 to 5°C, and then they were filtered. Dichloromethane was distilled off and the resultant products were washed several times with dry diethyl ether and dried. The three synthesized PNSs were given the abbreviations I1, I2, and I3 as illustrated in **Scheme 1**.

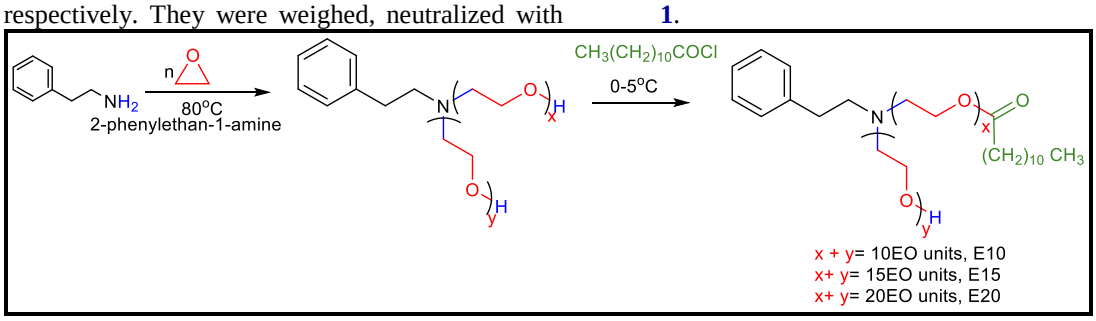

Scheme 1: Synthesis of polymeric nonionic surfactants.

2.3. Spectroscopic analysis

FTIR, MS and ^{1}H, ^{13}C-NMR were used to validate the chemical structure of the synthesized compounds. The IR spectra (KBr, ν cm) were obtained using a Perkin Elmer-FT-IR 1615, Waltham, MA, USA. NMR spectra were measured in (DMSO-d6) on a Bruker Avance (III) NMR spectrometer 400 MHz; ^{1}H & ^{13}C-NMR at 400, 100 MHz respectively: (Bruker, Switzerland). Thermo Scientific GCMS model ISQ was also employed to obtain the mass spectra at 70 eV.

2.4. Interfacial tension measurements

Theta optical Tensiometer (Attension-Biolin Scientific Company) was employed at 25°C to investigate the interfacial tension of different molar concentrations for the prepared PNSs (I1, I2, and

I3) in crude oil. The device specifications and method of work were previously stated [18]. Various interfacial properties and thermodynamic parameters such as γ_{cmc}, CMC, π_{cmc}, Γ_{max}, A_{min}, ΔG_{mic}, and ΔG_{ads} were measured and calculated as illustrated previously [19].

2.5. Cold flow performance tests

The maximum temperature at which the crude oil specimen lacks fluidity is defined as a solid point (SP) [20]. It is an important measure that reflects the cold flow behavior of WCO [21]. Therefore, in this study, SP was determined by utilizing the SYD-510F1 multipurpose low-temperature tester in accordance with GB/T510 [22]. The SP assessment was performed 3 times, and the mean value is deemed the final value. Then, the solid point depression (ΔSP) for each PNS and their blends was calculated for various dosages using the following Eq. (1) [23]:

$$\Delta SP = SP \text{ of untreated WCO} - SP \text{ of treated WCO} \quad (1)$$

2.6. Viscosity measurements

Rheological measurements were performed for untreated and treated WCO samples with a dosage of 1000 ppm from the commercial additive, PNSs, and their blends at a constant shear rate of 5 s^{-1} and a temperature range from 10 to 50°C [13] using the Brookfield DV-II+ programmable viscometer operating instructions manual no. M/97-164-D1000. Then, the reducing viscosity ratio (RVR) of WCO was calculated from the formula (2):

$$RVR = \beta_0 - \beta / \beta_0 \times 100\% \quad (2)$$

Where; β_0 denoted the viscosity of untreated WCO and β the viscosity of treated WCO.

2.7. Photomicrographic inspection.

Photomicrographic inspection of wax crystallization characteristics of untreated and treated WCO samples with the dosage of 1000 ppm was taken using an Olympus polarizing microscope model BHSP equipped with an automated camera in 35 mm format. It was connected to a cooling thermostat to regulate the temperature of the examined sample on the microscope slide. The magnification applied was 100X.

3. Results and Discussion

3.1. Affirmation of chemical composition

3.1.1. Ethoxylated 2-phenylethan-1-amine

FT-IR (KBr, ν_{max}) (Fig. 1) of ethoxylated 2-phenylethan-1-amine E20 (as a representative sample for the prepared ethoxylated compounds E10 and E15) revealed the apparition of two new distinctive bands; ether band (C–O–C) asymmetric stretching at 1109.9 cm^{-1} & broad band (OH) stretching at 3392.8 cm^{-1}. Aliphatic C–H at 2871.8, aromatic C–H, C=C at 3027.5, 1454.6 cm^{-1}, asym., sym. stretching C–N at 1249.8, 838.3 cm^{-1}. These inferences reveal that the functional groups C–O–C and OH were effectively integrated into 2-phenylethan-1-amine to yield ethoxylated 2-phenylethan-1-amine.

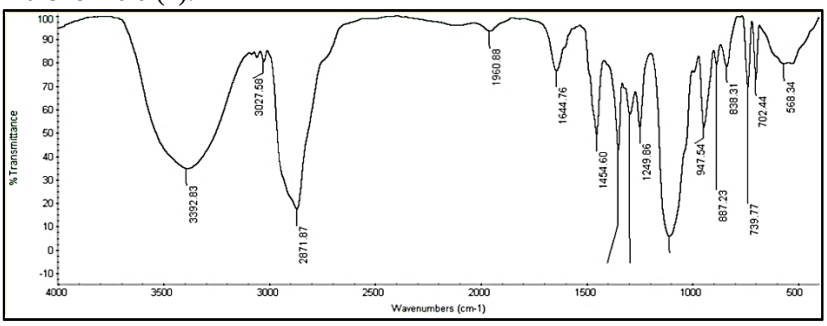

Fig. 1: FTIR of ethoxylated 2-phenylethan-1-amine E20.

Mass spectrum (Fig.2) of ethoxylated 2-phenylethan-1-amine (E10) exhibited a molecular ion peak at m/z 561.5 (30.6 % $C_{28}H_{51}O_{10}N$) and other significant peaks at 344.5 (100.6 % $C_{18}H_{34}O_5N$), 215.8 (29.4 % $C_{10}H_{16}O_5$), 252.6 (45.7 % $C_{14}H_{23}O_3N$), and 44.2 (7.3 % C_2H_4O). As displayed in Fig. 2, a molecular ion peak at m/z 561.5 verifies the existence of 10 units of EO in ethoxylated 2-phenylethan-1-amine (E10).

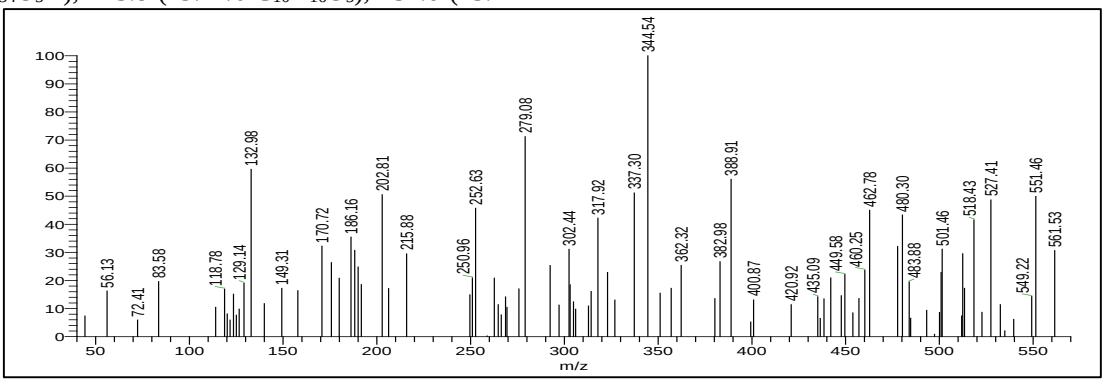

Fig. 2: Mass spectrum of ethoxylated 2-phenylethan-1-amine E10.

^{1}H-NMR spectrum (DMSO d_6) of E20 (**Fig. 3**) demonstrated various peaks at δ =4.5 ppm (1H, OCH_2CH_2O**H**); δ =3.6 ppm (2H, OCH_2C**H$_2$**OH); δ =3.5 ppm (2H, OC**H$_2$**C**H$_2$**O); δ =3.4 ppm (2H, CH_2C**H$_2$**NC**H$_2$**CH_2O); δ = 2.6 ppm (2H, C**H$_2$**$CH_2NCH_2CH_2O$); δ =7.2, 7.3 ppm (5H, Ar- **H**).

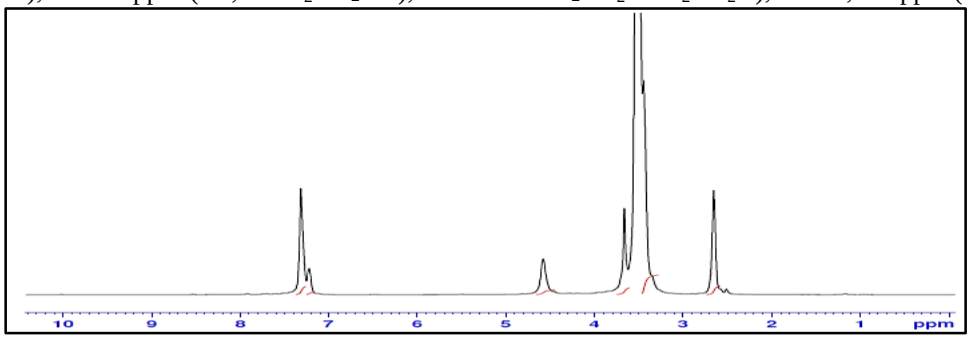

Fig. 3: ^{1}HNMR spectrum of ethoxylated 2-phenylethan-1-amine E20.

^{13}C-NMR spectrum (DMSO d_6) of E20 (**Fig. 4**) illustrates peaks at δ = 60.7 ppm attributable to carbon of (OCH_2**C**H_2OH**)**, δ = 72.7 ppm for (O**C**H_2CH_2OH), δ = 70.1 ppm for (O**C**H_2- CH_2O)), δ = 69.7 ppm for (O**C**H_2CH_2N-), δ = 53.7 ppm for (OCH_2**C**H_2N-), δ = 59.3 ppm for (N **C**H_2CH_2-ph), δ = 39.9 ppm for (N CH_2**C**H_2-ph), δ = 127.0- 140.2 ppm for (6PhC).

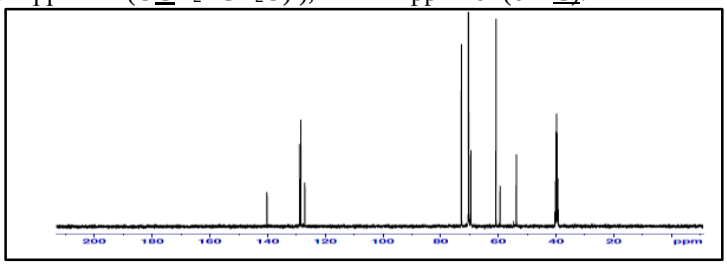

Fig. 4: ^{13}CNMR spectrum of ethoxylated 2-phenylethan-1-amine E20.

3.1.2. Esterification of polyoxyethylene 2-phenylethan-1-amine laurate.

FT-IR (KBr, vmax) (**Fig. 5**) spectrum of compound I3 (as a representative sample for the prepared compounds I1 and I2) confirmed the existence of a characteristic band; ester band (C=O) stretching at 1731.8 cm^{-1}. Aliphatic C–H at 2864.4, 2922.08 cm^{-1}, ether band (C–O–C) asymmetric stretching at 1107.6 cm^{-1}, broad band (OH) stretching at 3416.1 cm^{-1}. Aromatic C=C at 1460.1 cm^{-1}, asym., sym. stretching C–N at 1249.7, 842.7 cm^{-1}.

Mass spectrum (**Fig.6**) of **I1** exhibited a molecular ion peak at m/z 743.8 (19.9 % $C_{40}H_{73}O_{11}N$) and other significant peaks at 440.6 (100.0 % $C_{20}H_{40}O_{10}$), 163.8 (33.9 % $C_{10}H_{13}ON$), and 82.8 (40.8 % C_6H_{10}). The mass spectrum analysis affirmed the chemical composition of the synthesized **I1**.

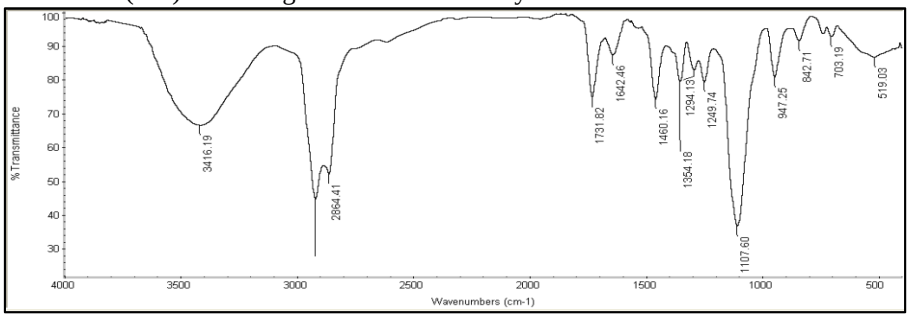

Fig. 5: FTIR spectrum of I3.

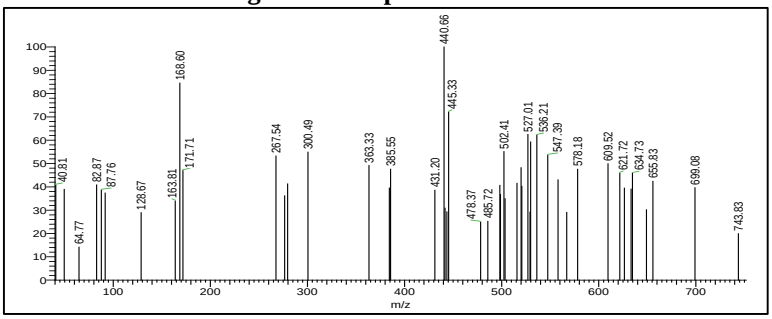

Fig. 6: Mass spectrum of I1.

^{1}H-NMR (DMSO d_6) spectrum I3 (**Fig. 7**) revealed various peaks at δ = 0.84 ppm (3H, C**H**$_3$); δ =1.2 ppm (16H, (C**H**$_2$)$_8$); δ =1.5 ppm (2H, C**H**$_2$CH$_2$C=O); δ =2.1 ppm (2H, C**H**$_2$C=O); δ =4.1 ppm (2H,O=C–OC**H**$_2$CH$_2$O); δ =3.7 ppm (2H,O=C–OCH$_2$C**H**$_2$O); δ=3.5 ppm (2H,OC**H**$_2$C**H**$_2$O); δ=2.2 ppm (2H, NC**H**$_2$CH$_2$O); δ = 2.5 ppm (2H, C**H**$_2$CH$_2$N); δ = 2.8 ppm (2H, CH$_2$C**H**$_2$N); δ = 3.9 ppm (OCH$_2$C**H**$_2$OH**)**; δ = 4.6 ppm (CH$_2$O**H**); δ =7.2- 7.4 ppm (5H, Ar-**H**).

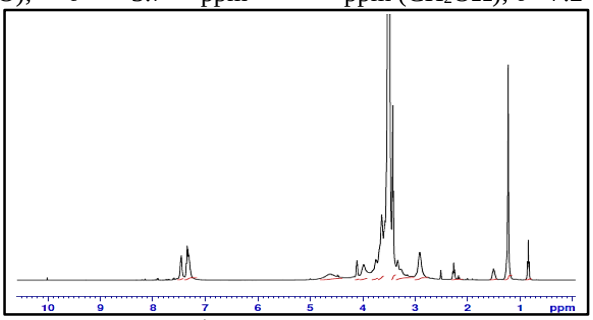

Fig. 7: ^{1}HNMR spectrum of I3.

^{13}C-NMR (DMSO d_6) spectrum of I3 (**Fig. 8**) illustrates peaks at δ = 14.2 ppm attributable to carbon of (**C**H$_3$**)**; δ = 22.5 ppm for (**C**H$_2$CH$_3$); δ = 31.7 ppm for (**C**H$_2$CH$_2$CH$_3$); δ = 29.5 ppm for ((**C**H$_2$)$_6$ CH$_2$CH$_3$); δ = 24.9 ppm for (**C**H$_2$CH$_2$C=O); δ = 33.9 ppm for (CH$_2$**C**H$_2$C=O); δ = 173.2 ppm for (CH$_2$CH$_2$**C**=O); δ = 63.4 ppm for (OCH$_2$**C**H$_2$C=O); δ = 66.0 ppm for (O**C**H$_2$CH$_2$C=O); δ = 60.7ppm for (OCH$_2$**C**H$_2$OH**)**, δ = 72.7 ppm for (O**C**H$_2$CH$_2$OH), δ = 70.1 ppm for (O**C**H$_2$- CH$_2$O), δ = 68.8 ppm for (O**C**H$_2$CH$_2$N-), δ = 53.1 ppm for (OCH$_2$**C**H$_2$N-), δ = 58.8 ppm for (N **C**H$_2$CH$_2$-ph), δ = 39.9 ppm for (N CH$_2$**C**H$_2$-ph), δ = 128.0- 134.9 ppm for (6Ph**C**).

3.2. Interfacial tension measurements and calculations

Various properties and parameters were measured, calculated, and gathered in **Tables 2** and **Fig. 9**. From the acquired data, it was observed that the three synthesized PNSs I1, I2 and I3 reduced the IFT between the water/WCO from 21 mN/m to 3, 2, and 1.5 mN/m respectively and I3 which possesses the largest number of ethylene oxide units (EO), exhibited the lowest IFT as their γ_{cmc} and CMCs values decreased by increasing the number of EO units incorporated. Also, a relationship between both Γ_{max} and A_{min} and the number of EO units was found. Where, with increasing the number of EO units, the values of Γ_{max} decreased while the A_{min} values increased. This can be attributed to the tendency of the PNSs to be adsorbed at the water/WCO interface.

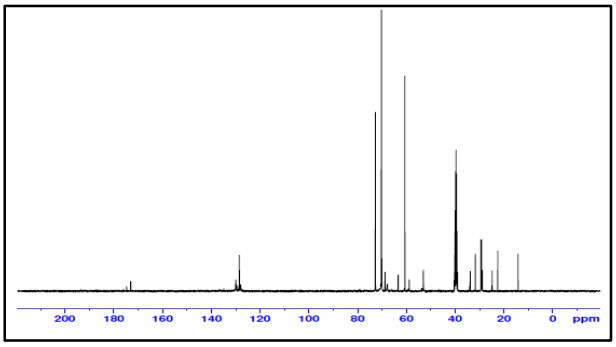

Fig. 8: ^{13}CNMR spectrum of I3.

Table 2: Interfacial tension parameters and thermodynamic properties of the prepared polymeric nonionic surfactants

Name	γ_{IFT} (mN m^{-1})	CMC (mol dm^{-3})	π_{cmc} (mN m^{-1})	Γ_{max} x 10^{10} (mol cm^{-2})	A_{min} (A^{o2} molecule^{-1})	ΔG_{mic} (kJ mol^{-1})	ΔG_{ads} (kJ mol^{-1})
I1	3	0.00125	18	1.12	147.85	-30.11	-31.94
I2	2	0.000625	19	1.077	154.12	-33.24	-35.16
I3	1.5	0.000521	19.5	0.989	167.72	-34.06	-36.03

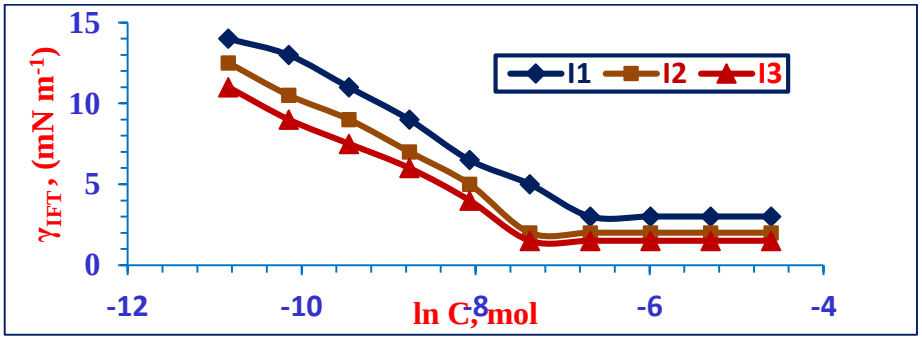

Fig. 9: Interfacial Tension (γ_{IFT}) vs. the Ln Concentrations of the I1, I2 and I3.

Also, the values of ΔG_{mic} and ΔG_{ads} for the synthesized PNSs were displayed in **Tables 2**. From those calculated data, it can be concluded that:

(a) Micellization & adsorption are spontaneous processes because the values of ΔG_{mic} and ΔG_{ads} are negative.
(b) The values of ΔG_{ads} are more negative than the values of ΔG_{mic} which suggest that the synthesized PNSs favor adsorption on the interfaces over micelle formation since the adsorption at interfaces resulted in a decrease in the system's free energy **[24]**.
(c) The ΔG_{ads} value of I3 is more negative than that of I1and I2 which indicates that I3 molecules adsorb more strongly on the interfaces.

3.3. Solid Point depression (ΔSP)

The solid points for untreated and treated WCO with the synthesized PNSs and their blends were measured for dosage range from 250 to 2000 ppm, and the corresponding depression in the solid point (ΔSP) was also calculated for each measurement as demonstrated in **Tables 3 and 4**. Variation in the dosage of the PNSs and their blends, the molar ratios of the blends, and the PNSs molecular structures are significant factors that impact the values of SP and ΔSP, which can be illustrated as follows in table 3.

3.3.1. Variation in the dosage

The values of SP and ΔSP for various dosages of the commercial additive and PNSs are depicted in **Table 3 and Fig. 10**. For all the PNSs except I1, it is apparent from the data that increasing the dosages from 250 ppm to 1000 ppm reduces the SP values and raises the corresponding values of ΔSP generally, which improves their activities as cold flow improvers and wax dispersants. However, with the successive increase in the PNSs dosages, the SP exhibited no change (from 1000 to 2000 ppm). The SP and ΔSP values of I3 for various dosages were better than those of I2, where I3 reduced the SP to 6°C and increased the ΔSP to 15 but the values of I2 were 9°C and 12. Clearly, a dosage of 1000 ppm which is close to the CMCs of the PNSs is the optimum dosage for enhancing the behavior of cold flow ability and wax dispersion, where most of the paraffin particles at this dosage were surrounded by surfactants molecules, preventing their aggregation and hence promoting higher inhibition of wax deposition. As a consequence, adding more surfactant molecules did not affect the SP reduction.

From **Table 3**, I2 and I3 give better depression of solid point than those obtained with the commercial sample (ΔSP_{1000} = 9°C).

Table3: Effect of commercial additive and individual PNS additives on the solid point of the waxy crude oil

PNS name	Concentration, ppm	SP,°C	ΔSP
*Blank	-	21	-
Com.	250	18	3
	500	15	6
	750	15	6
	1000	12	9
	2000	12	9
I1	250	21	0
	500	21	0
	750	21	0
	1000	18	3
	2000	18	3
I2	250	18	3
	500	15	6
	750	12	9
	1000	9	12
	2000	9	12
I3	250	15	6
	500	12	9
	750	9	12
	1000	6	15
	2000	6	15

*Blank = waxy crude oil

Table 4: Effect of mixed PNS additives on the solid point of the waxy crude oil

Mixed PNS name	Concentration ppm	SP,°C	ΔSP
I4 I1:I3 (1:1)	250	18	3
	500	15	6
	750	12	9
	1000	9	12
I5 I1:I3 (1:2)	250	15	6
	500	9	12
	750	9	12
	1000	6	15
I6 I2:I3 (1:1)	250	12	9
	500	9	12
	750	6	15
	1000	3	18
I7 I2:I3 (1:2)	250	9	12
	500	6	15
	750	3	18
	1000	0	21

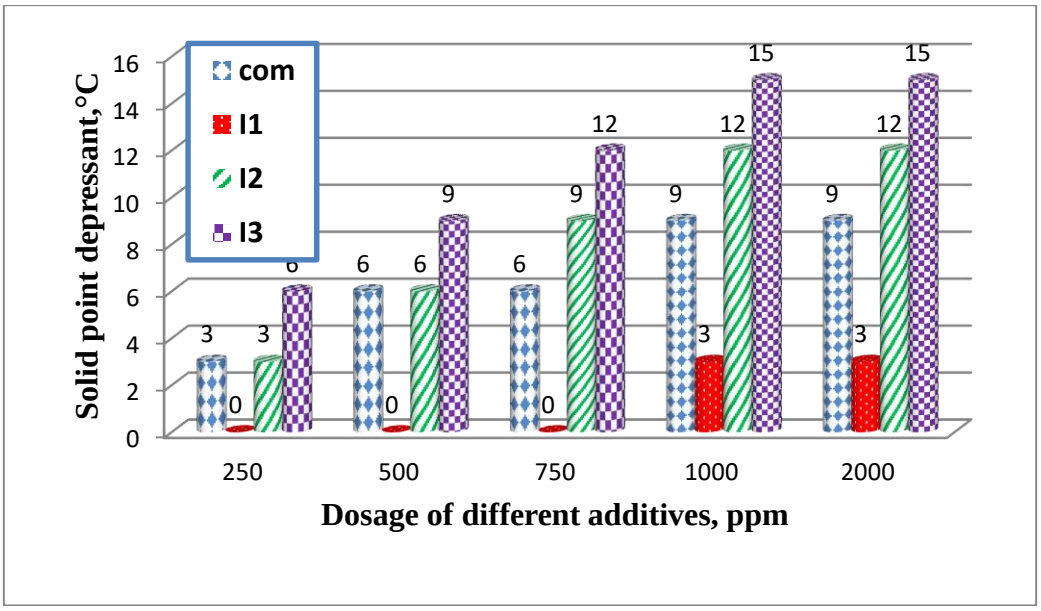

Fig. 10: Effect of different additives concentrations on the solid point of waxy crude oil.

The impact of various dosages of blended PNSs on the values of SP and ΔSP was similar to that of the PNSs as shown in **Table 4** and **Fig. 11**, where the SP values reduced with increasing the dosages while the ΔSP values raised. The blend I7 showed the best values of all blends with SP and ΔSP values equal to 0 °C and 21 respectively. This means that a synergistic effect takes place between the blended molecules which improves the adsorption and co-crystallization with the paraffin molecules through the nonpolar parts and increases their dispersion via the influence of the polar parts, where the polar parts inhibit the wax crystals´ growth and aggregation which advances the cold flow behavior and wax dispersion **[25]**.

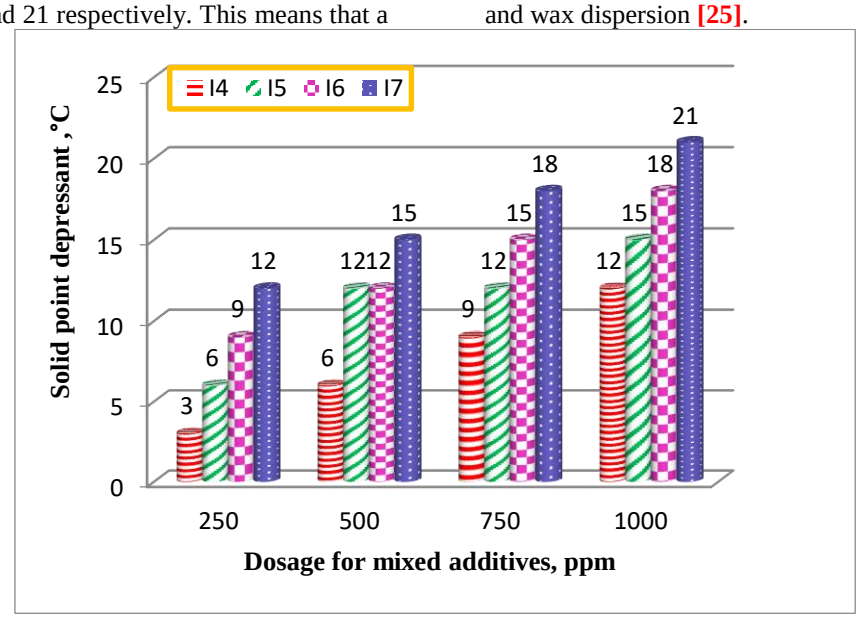

Fig. 11: Effect of mixed additives concentrations on solid point of waxy crude oil.

3.3.2. PNSs molecular structures

The molecular structure effect of the PNSs on the SP and ΔSP of WCO can be elicited from **Table 3 and Fig. 10**. The findings reveal that the SP values decrease and hence the ΔSP increase as the polyoxyethylene chain length of the PNS enlarges, where the values of the SP for I1, I2, and I3 at 1000 ppm were 18, 9, and 6°C respectively, while the corresponding ΔSP values were 3, 12 and 15. That may be attributed to an enhancement of the adsorption and co-crystallization processes by increasing the polar group content (ethylene oxide units), which hinders the growth of wax crystals and improves fluidity **[15]**.

3.3.3. Molar ratios of the blends

The PNS I3 has the most efficient values of SP and ΔSP at various dosages, so it was blended with I1 and I2 with various molar ratios. The impact of that blending on the SP and ΔSP values of treated WCO were recorded and figured in **Table 4 and Fig. 11**.

The performance of I1 which has no noticeable effect on SP and ΔSP values was improved when mixed with I3 in different molar ratios as seen from the results of I5 with blending ratio 1:2 (SP=6°C and ΔSP=15 at 1000 ppm). Also, the performance of I2 was improved when mixed with I3 in different ratios. As the molar ratio of I3 was increased in the blend better values of SP and ΔSP were exhibited. So, the blend I7 exhibited a better result than the blend I6 and also exhibited the best results of blends and PNSs. Generally, the blending played a positive effect on the resulted data owing to the synergistic effects between the blended surfactants, especially for the blend I7 which contains highly polar groups with larger polyoxyethylene chain length. All the blends of PNSs decreased wax crystal super-saturation in WCO and considerably enhanced wax crystal solubility. As a consequence, the crystal growth strategy and growth effectiveness were altered, which impeded wax crystals' creation [26].

3.4. Rheological measurements of untreated and treated WCO

The viscosity for untreated and treated WCO with commercial additive, the synthesized PNSs, and their blends (the dosage was 1000 ppm) was measured and the values of RVR were calculated as demonstrated in Table 5. Commercial additive, PNSs, and their blends reduced the viscosity of WCO and the corresponding RVR values were not less than 40%. For the individual PNSs I1, I2, I3, and commercial additive the RVR values were 40.6, 44.4, 50.6, and 49.3% respectively, whereas the RVR values for the blends I4, I5, I6, and I7 were 51.6, 55.2, 53.5 and 60.5% respectively. Figure 12 depicts the apparent viscosities of both untreated and treated WCO with I3 and I7 WDs at various temperatures. The viscosities of untreated and treated WCO consistently reduced as the temperature goes up for all curves, such behavior was attributable to the thermal impact [21]. Moreover, the viscosity values of WCO dosed with I3 and I7 WDs were lower than those of untreated and treated WCO with toluene, despite the toluene solvent having a minimal effect on the viscosity of WCO as displayed in Fig. 12. I7 WD performed better than I3 WD across the entire temperature range, indicating that the viscosity decline behavior was controlled by the excessive intensity of interaction between I7 and WCO components.

Table 5: Viscosity reduce rate of waxy crude oil at 1000ppm from commercial additive individual and mixed PNS additives

Additives	Com.	I1	I2	I3	I4	I5	I6	I7
Viscosity reduce rate %	49.3	40.6	44.4	50.6	51.6	55.2	53.5	60.5

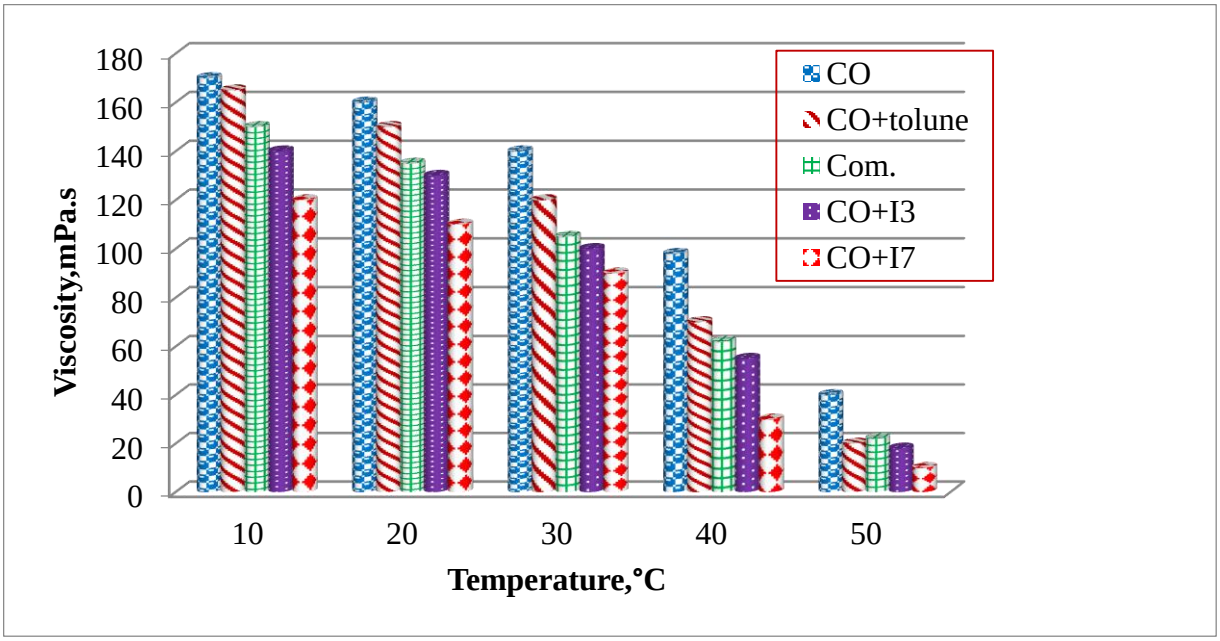

Fig. 12: Apparent viscosity of untreated crude oil and treated with Com., I3, and I7 additives.

3.5. Photomicrographic analysis

Figure 13 represented the photomicrographic observation of untreated and treated WCO with a 1000 ppm dosage of I1, I2, I3, and blend I7. As seen in Fig. 13a, huge and asymmetrical wax crystals were produced in WCO when the temperature dropped to 0°C. Wax crystals grew in a 3D network structure, wrapping the liquid crude oil and reducing its fluidity. While the PNSs and the blend I7 were applied to WCO as seen in Fig. 13b–e, wax crystal sizes diminished and became irregular (acting as wax dispersants), which impeded the porous network creation. It suggested that the PNSs and the blend I7 have

significantly varied the morphology of the crystalline phase and reduced the system energy by altering the crystallization attitude of WCO [27,28]. The long chains of the PNSs and the blend I7 interacted and co-crystallized with paraffin to produce multiple crystallization nuclei. As the temperature dropped, additional paraffin in WCO progressively crystallized out. Concurrently, the polar moieties of the PNSs and the blend I7 penetrated crystal lattice and restricted the generation of bigger wax crystals, promoting dispersibility, reducing wax crystal size, and hindering the 3D network structure creation (as seen in Fig. 13b–e). The blend I7 (with the molar ratio 1I2:2I3) has presented better morphology in the micrographic analysis as illustrated in Fig. 13e which may be attributed to the synergistic effect of the two blended I2 and I3.

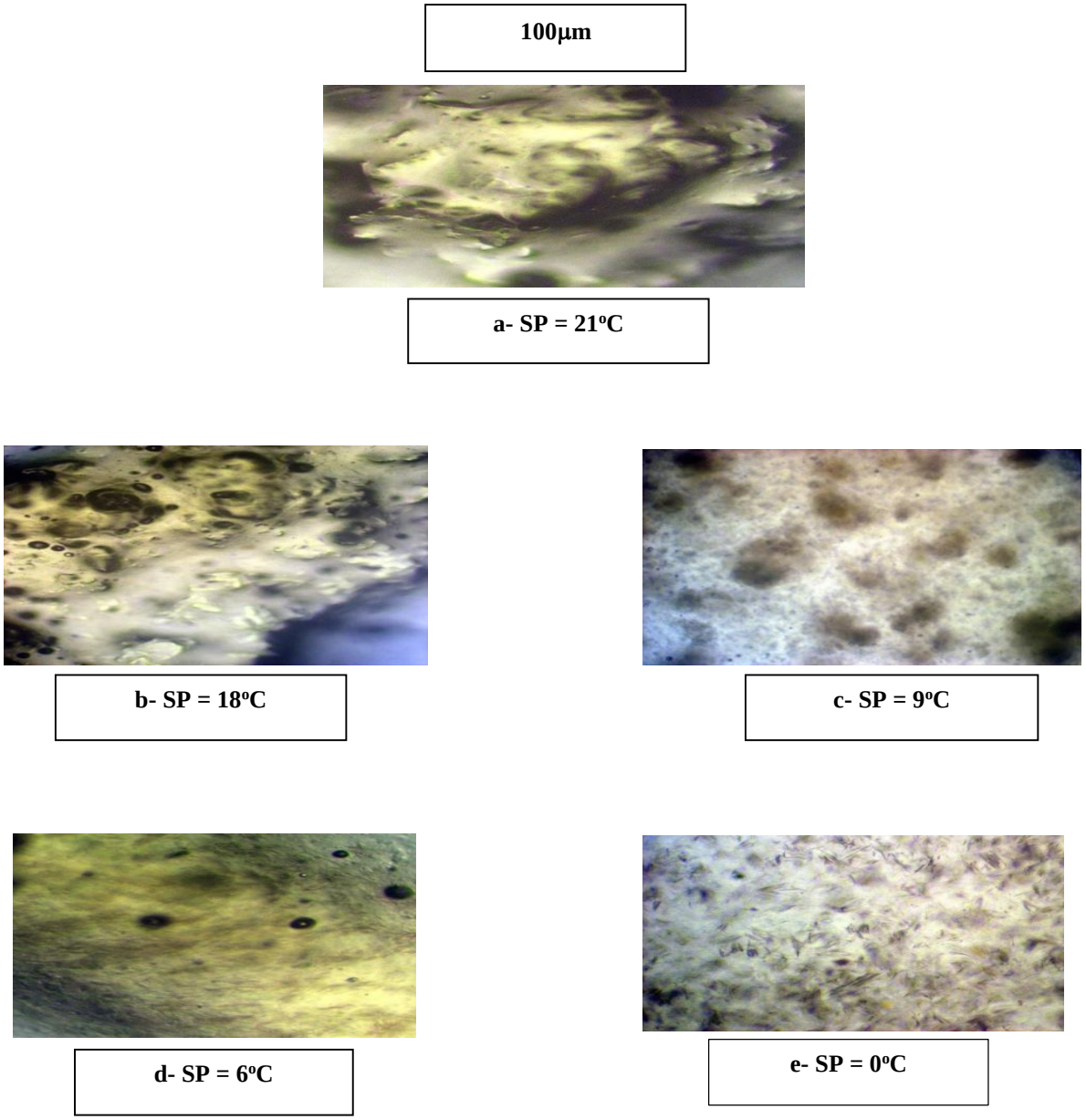

Fig. 13: Photomicrographs of a: untreated crude oil (CO), b:(CO)+1000ppm I1, c: (CO) + 1000ppm I2 , d: (CO)+1000ppm I3 and e: (CO)+1000ppm I7

3.6. Inspection of the PNS depressing mechanism

The mechanism of the PNS on the ΔSP of WCO was studied at the molecular level based on the findings of the experiments. Figure 14 illustrates that the straight alkanes in the untreated WCO effectively precipitated and aggregated into a 3 D network structure at low temperatures, resulting in crude oil solidification. For PNS-treated WCO, the PNS molecular structure is typically composed of a linear hydrocarbon chain and polar group segment. As a result, the PNS generally inhibits wax deposition via linear hydrocarbon chains that interrelate with wax crystals and hence, disperse them in crude oil using the polar groups to avoid aggregation.

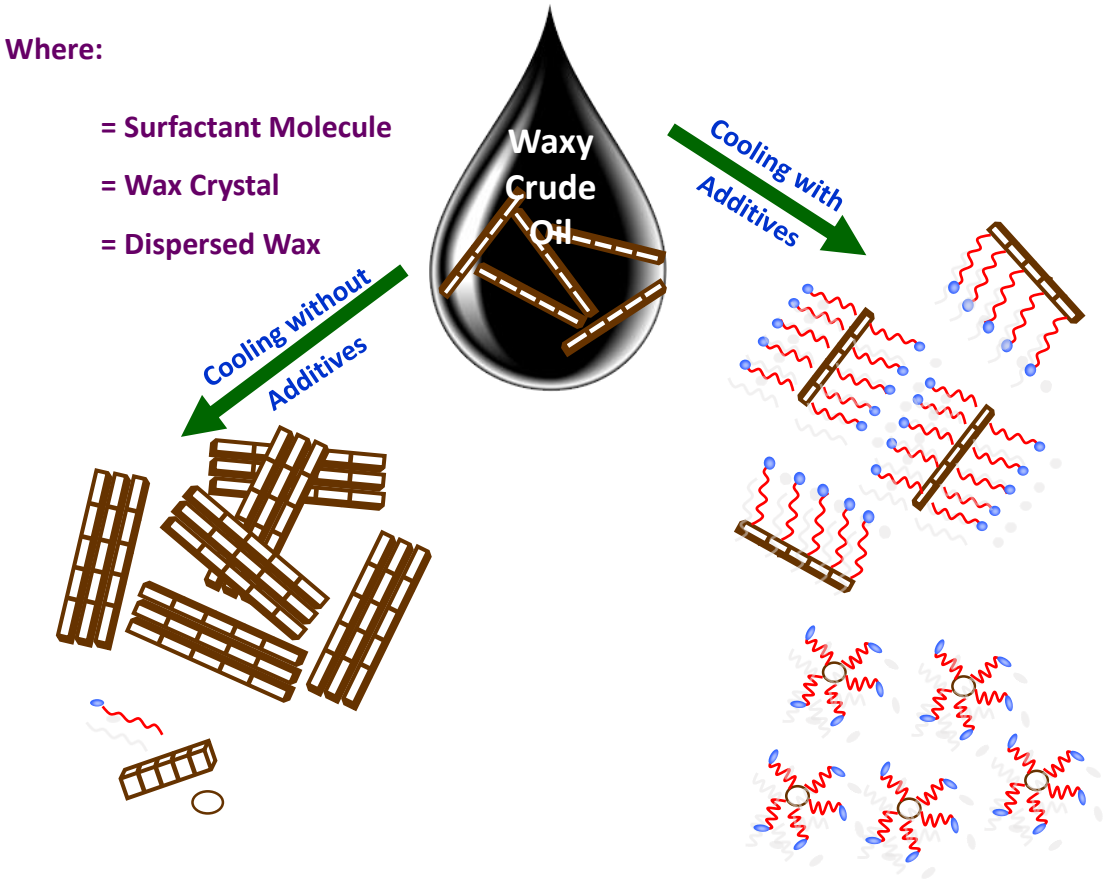

Fig. 14: Mechanism of PNS on the solid point depression of waxy crude oil

Conclusions

Polymeric nonionic surfactants series based on 2-phenylethan-1-amine was synthesized, characterized, and employed as an efficient SP depressant for waxy crude oil. IFT measurements were conducted to assess the surface parameters of the PNSs. Individual additive I3 exhibited the best depression on the SP of crude oil where the ΔSP reached a maximum of 15°C. To improve the cold flow properties of crude oil, I3 additive mixed in different molar ratios with I1 and I2 ($1I_1$:$1I_3$,$1I_1$:$2I_3$,$1I_2$:$1I_3$ and $1I_2$:$2I_3$) respectively, and used to depress SP of crude oil. Among these combined PNSs, the I7 additive showed the best inhibitory effect which exerted the lowest ΔSP was 21°C. With increasing the concentration of the additives, an increase in their activity was obtained and as a result, a great depression of solid point was achieved. In terms of rheological performance, I7 performed better than I3 across the entire temperature range, decreasing crude oil viscosity and improving its flowability**.** The obtained findings were compared to commercial solid point depression; the results revealed that synthesized PNS with crude oil provided a better solid point depression than the commercial sample. Polarizing optical microscopy was performed to assess the interacting mechanisms of PNSs on the solid point depression of WCO.

References

[1] K. Bybee, Heavy Oil: Combustion-Tube Experiments Show Heavy-Oil-Production Increase With Addition of Catalyst, J. Pet. Technol. 60 (2008) 88–90. https://doi.org/10.2118/0308-0088-JPT.

[2] R.N. Tuttle, High-Pour-Point and Asphaltic Crude Oils and Condensates, J. Pet. Technol. 35 (1983) 1192–1196. https://doi.org/10.2118/10004-PA.

[3] S.M. Ahmed, T.T. Khidr, D.A. Ismail, Effect of gemini surfactant additives on pour point depressant of crude oil, J. Dispers. Sci. Technol. 39 (2018) 1160–1164. https://doi.org/10.1080/01932691.2017.1385483.

[4] A. Al-Sabagh, M. Sabaa, G. Saad, T.T. Khidr, T.M. Khalil, Synthesis of polymeric additives based on itaconic acid and their evaluation as pour point depressants for lube oil in relation to rheological flow properties, Egypt. J. Pet. 21 (2012) 19–30. https://doi.org/10.1016/j.ejpe.2012.02.003.

[5] E.A. Soliman, M.R. Elkatory, A.I. Hashem, H.S. Ibrahim, Synthesis and performance of maleic anhydride copolymers with alkyl linoleate or

tetra-esters as pour point depressants for waxy crude oil, Fuel. 211 (2018) 535–547. https://doi.org/https://doi.org/10.1016/j.fuel.2017.09.038.

[6] Recent advances on mitigating wax problem using polymeric wax crystal modifier, J. Pet. Explor. Prod. Technol. 5 (2014) 1–11. https://doi.org/10.1007/s13202-014-0146-6.

[7] T.T. Khidr, S.M. Ahmed, The effect of cationic surfactant additives on flow properties of crude oil, Pet. Sci. Technol. 34 (2016) 1219–1225. https://doi.org/10.1080/10916466.2016.1194861.

[8] Y. Ren, L. Fang, Z. Chen, H. Du, X. Zhang, Synthesis and Evaluation of Grafted EVAL as Pour Point Depressant for Waxy Crude Oil, Ind. Eng. Chem. Res. 57 (2018) 8612–8619. https://doi.org/10.1021/acs.iecr.8b01169.

[9] A. Erceg Kuzmić, M. Radošević, G. Bogdanić, V. Srića, R. Vuković, Studies on the influence of long chain acrylic esters polymers with polar monomers as crude oil flow improver additives, Fuel. 87 (2008) 2943–2950. https://doi.org/https://doi.org/10.1016/j.fuel.2008.04.006.

[10] aziza S. El-Tabei, E. Arafa, taisir Khidr, Studies of Synthesized Nonionic Gemini Surfactant Based On Sulfonamide Moiety as Flow Enhancing Additive of Waxy Crude Oil, Egypt. J. Chem. 64 (2021) 1495–1502. https://doi.org/10.21608/ejchem.2020.47823.3000.

[11] M. Xie, F. Chen, J. Liu, T. Yang, S. Yin, H. Lin, Y. Xue, S. Han, Synthesis and evaluation of benzyl methacrylate-methacrylate copolymers as pour point depressant in diesel fuel, Fuel. 255 (2019) 115880. https://doi.org/https://doi.org/10.1016/j.fuel.2019.115880.

[12] G. Chen, Z. Zhou, X. Shi, X. Zhang, S. Dong, J. Zhang, Synthesis of alkylbenzenesulfonate and its behavior as flow improver in crude oil, Fuel. 288 (2021) 119644. https://doi.org/https://doi.org/10.1016/j.fuel.2020.119644.

[13] X. Gu, F. Zhang, Y. Li, J. Zhang, S. Chen, C. Qu, G. Chen, Investigation of cationic surfactants as clean flow improvers for crude oil and a mechanism study, J. Pet. Sci. Eng. 164 (2018) 87–90. https://doi.org/https://doi.org/10.1016/j.petrol.2018.01.045.

[14] N. Hazrati, M. Abdouss, A.A. Miran-Beigi, A.A. Pasban, Long Chain Alkylated Ionic Liquids as Pour Point Depressant and Rheology Improver for Crude Oil, Pet. Chem. 61 (2021) 206–213. https://doi.org/10.1134/S0965544121020079.

[15] O.A.A. El-Shamy, T.T. Khidr, M.M. Doheim, Polymeric Nonionic Surfactants as a Pour Point Depressant, Pet. Sci. Technol. 32 (2014) 2195–2202. https://doi.org/10.1080/10916466.2013.774015.

[16] S. Banerjee, R. Kumar, A. Mandal, T.K. Naiya, Use of a Novel Natural Surfactant for Improving Flowability of Indian Heavy Crude Oil, Pet. Sci. Technol. 33 (2015) 819–826. https://doi.org/10.1080/10916466.2015.1014961.

[17] S. Yi, J. Zhang, Shear-Induced Change in Morphology of Wax Crystals and Flow Properties of Waxy Crudes Modified with the Pour-Point Depressant, Energy & Fuels. 25 (2011) 5660–5671. https://doi.org/10.1021/ef201187n.

[18] M.R. Noor El-Din, M.R. Mishrif, A. El-Tabey, A study on the effect of dynamic interfacial tension on the stability of nano-emulsified diesel, J. Mol. Liq. 254 (2018) 39–46. https://doi.org/https://doi.org/10.1016/j.molliq.2018.01.065.

[19] A.S. El-Tabei, A.E. El-Tabey, E.A. El-Sharaky, Novel synthesized polymeric surfactants additives based on phenethylamine as an emulsion breaker for water droplet coalescence in naturally Egyptian crude oil emulsion, J. Mol. Liq. 338 (2021) 116779. https://doi.org/https://doi.org/10.1016/j.molliq.2021.116779.

[20] B. Yao, L. Wang, F. Yang, C. Li, Y. Zhao, Effect of Vinyl-Acetate Moiety Molar Fraction on the Performance of Poly(Octadecyl Acrylate-Vinyl Acetate) Pour Point Depressants: Experiments and Mesoscopic Dynamics Simulation, Energy & Fuels. 31 (2017) 448–457. https://doi.org/10.1021/acs.energyfuels.6b02688.

[21] ASTM, Standard test method for pour point of petroleum products, (2017).

[22] GB/T510-2018, Standard Press of China, Determination of solidification point for petroleum products, (2018).

[23] T. Yang, S. Yin, M. Xie, F. Chen, B. Su, H. Lin, Y. Xue, S. Han, Effects of N-containing pour point depressants on the cold flow properties of diesel fuel, Fuel. 272 (2020) 117666. https://doi.org/https://doi.org/10.1016/j.fuel.2020.117666.

[24] A.M. Al-Sabagh, H.M. Abd-El-Bary, R.A. El-Ghazawy, M.R. Mishrif, B.M. Hussein, Surface active and thermodynamic properties of some surfactants derived from locally linear and heavy alkyl benzene in relation to corrosion inhibition efficiency, Mater. Corros. 62 (2011) 1015–1030. https://doi.org/https://doi.org/10.1002/maco.201006017.

[25] J. Zhang, C. Wu, W. Li, Y. Wang, H. Cao, DFT and MM calculation: the performance mechanism of pour point depressants study, Fuel. 83 (2004) 315–326. https://doi.org/https://doi.org/10.1016/j.fuel.2003.08.010.

[26] H. Lin, S. Yin, B. Su, Y. Xue, S. Han, Research on combined-pour point depressant of methacrylate-acrylamide copolymers and ethylene-vinyl acetate copolymers for diesel fuel, Fuel. 290 (2021) 120002. https://doi.org/https://doi.org/10.1016/j.fuel.2020.120002.

[27] S.M. Ahmed, T.T. Khidr, E.S. Ali, Preparation and evaluation of polymeric additives based on poly(styrene-co-acrylic acid) as pour point depressant for crude oil, J. Dispers. Sci. Technol. (2021) 1–8. https://doi.org/10.1080/01932691.2021.1878038.

[28] B. Deka, R. Sharma, V. Mahto, Synthesis and performance evaluation of poly (fatty esters-co-succinic anhydride) as pour point depressants for waxy crude oils, J. Pet. Sci. Eng. 191 (2020) 107153. https://doi.org/https://doi.org/10.1016/j.petrol.2020.107153.